1 **Toward performance improvement of supersulfated cement by nano silica:**

2 **Asynchronous regulation on the hydration kinetics of silicate and aluminate**

3 Heng Chen[a], Pengkun Hou[ab], Xiangming Zhou[b], Leon Black[c], Samuel Adu-Amankwah[c], Pan Feng[d],

4 Na Cui[e], Michał A. Glinicki[f], Yamei Cai[g], Shipeng Zhang[g], Piqi Zhao[a], Qinfei Li[a], Xin Cheng[a]

5 [a]Shandong Provincial Key Lab for the Preparation & Measurement of Building Materials, University of Jinan,

6 Jinan, Shandong 250022, China

7 [b]Department of Civil & Environmental Engineering, Brunel University London, Uxbridge, Middlesex UB8 3PH,

8 UK

9 [c]School of Civil Engineering, University of Leeds, Woodhouse Lane, LS29JT, UK

10 [d]School of Materials Science and Engineering, Southeast University, Nanjing, Jiangsu 211189, China

11 [e]School of Civil Engineering and Architecture, University of Jinan, Jinan, Shandong 250022, China

12 [f]Institute of Fundamental Technological Research, Polish Academy of Sciences, Pawinskiego 5b, 02-106 Warsaw,

13 Poland

14 [g]Department of Civil and Environmental Engineering, The Hong Kong Polytechnic University, Hong Kong

15 Abstract

16 Supersulfated cement (SSC) is a traditional low-carbon cement, but its slow hydration and

17 strength development have limited its practical applications. Nano silica (NS) was used to activate the

18 hydration of SSC by taking advantage of its ability to regulate silicate and aluminate reactions. The

19 mechanical performance of various mixes was determined, as a function of sulfation degree and NS

20 addition, as pore structure, phase assemblage, hydration degree, and microstructure. Results showed

21 that NS improves the hydration degree of slag, densifies the microstructure, and significantly increases

22 both early- and late-age compressive strength. The enhancement was attributed to its effects on the

23 hydration of slag in SSC: delaying ettringite formation but promoting C-(A)-S-H precipitation,

24 reducing microporosity. This study reveals the critical role of the regulation of hydration kinetics of

25 silicate and aluminate in controlling the performance of SSC as NS does.

26 **Keywords:** Supersulfated cement, nano silica, gypsum content, mechanical property, microstructure

1. Introduction

CO$_2$ emissions associated with Portland cement production is a major sustainability challenge to the cement industry. Low-carbon alternatives such as calcium sulfoaluminate cement (CSA) [1], supersulfated cement (SSC) [2], have been developed to partially replace Portland cement, and so reduce the CO$_2$ emissions of the cement industry. As a classic low-carbon cement, SSC, has attracted attention recently, thanks to its ultra-low clinker content, utilization of solid wastes, and excellent sulfate resistance [3-5]. Similar to CSA, the main hydration products of SSC are ettringite (AFt) and aluminum incorporated calcium silicate hydrates (C-(A)-S-H) [6]. Unlike CSA, practical application of SSC is limited due to its lower early strength.

Low early-age strength of SSCs has been attributed to the slow dissolution of slag [7, 8]. Early-age strength can be improved by increasing the amount of Portland cement, but this can decrease the long-term compressive strength of hardened SSC mortars [1, 9]. Although this phenomenon has not been resolved completely, possible reasons could be inhibition of slag dissolution by the preferred precipitation of AFt [9] or hydrotalcite[10] on the surface of slag in SSC with high alkali content in the presence of excess of Portland cement. On top of this, it has also been found that the addition of alkalis, such as KOH or NaOH, or alkali sulfate cannot increase the strength of SSC [9, 11], although Briki et al. showed that slag has much higher reactivity in NaOH solution than in cement paste [12]. There seems existing an optimal pH range for the hydration of SSC, especially for the precipitation of AFt [1, 2]. Recently, sodium lactate had been found to increase the compressive strength of SSC [3, 11] and it was proposed that the chelation of lactate on the surface of slag could promote the breaking of silicon-oxygen network [3].

From above, most of the published literature on SSC appears to focus on methods for promoting the dissolution of slag, in order to accelerate the hydration of SSC. However, from the principle of chemical equilibrium, both the dissolution of reactants and the precipitation of reaction products are frequently coupled with each other and both of them are responsible for the reaction rate [8], as in the Portland cement system [13, 14]. Therefore, accelerating the precipitation of hydration products could be another way to promote the hydration process. It has long been found that the addition of nucleation seeds would increase the early strength of cementitious materials, such as calcium silicate hydrate (C-

S-H) seeds in Portland cement systems [15], and AFt seeds in SAC system [16]. Similar to C-S-H, nano silica (NS) has also been shown to provide nucleation sites for C-S-H and accelerate the hydration kinetics of Portland cement at early age [17, 18]. Since C-(A)-S-H is one of the two main hydration products of SSC [2], the addition of nano silica could accelerate the hydration of SSC. In fact, Ma et al. [19] found 3 *wt*.% of NS increased the compressive strength of SAC at 8 h, 1 day, and 56 days by ~42%, ~38%, and ~65%, respectively through promoting hydration of SAC and densifying its microstructure. Since SSC shares similar hydration products with SAC, the addition of NS could enhance the hydration of SSC. Li at al. [20] found 1wt.% of NS increased the compressive strength of CSA/Portland cement at 2 hours and 28 days by ~42% and ~20%, respectively. In addition, Hou et al. [21] proposed that NS has contrary influence on the precipitation of AFt and C-(A)-S-H in the system of $CaSO_4$-C_3S-C_3A. Thus, NS could modify the ratio of the two main hydration products (C-(A)-S-H and AFt) which could further affect the hydration and performance of SSC.

Therefore, to reveal the effect of NS on SSC hydration and performance, SSC was prepared with either 4 or 10% gypsum and with part of the slag replaced by NS (3 *wt*.% of total mass). It is shown that NS significantly promotes the hydration kinetics, densifies the microstructure, and increases the mechanical strength of SSC. The role of NS in the regulation of aluminate and silicate precipitation is also discussed.

2. Material and methods

2.1. Materials

The main components of SSC are ground granulated blast furnace slag, cement and gypsum. The chemical and mineral compositions of the slag and Portland cement (Chinese P·I 42.5) are presented in **Table 1**. It can be noted that it is an acid slag, indicating its low reactivity. Gypsum used was of analytical grade. The NS had a diameter of 7-40 nm, and a specific surface area of 380 m^2/g. The particle size distributions of slag, Portland cement and gypsum are shown in **Figure 1**. The naphthalene superplasticizer from Sobute was used for preparing cement pastes and mortars. Chinese standard sand was used in the mortars. In addition, limestone powder with particle size less than 150 um, was added in SSC, considering its stabilization effect on AFt and synergetic effect with aluminosilicate [22, 23].

Table 1. Chemical compositions of Portland cement and GGBS in this study

	CaO	SiO$_2$	Al$_2$O$_3$	SO$_3$	Fe$_2$O$_3$	MgO	LOI*	SSA (m^2/Kg)
Portland cement	64.39	21.88	4.31	2.56	3.47	1.72	1.42	340
GGBS	30.20	32.78	17.55	2.30	1.45	6.36	9.36	531

LOI*: Lost on ignition.
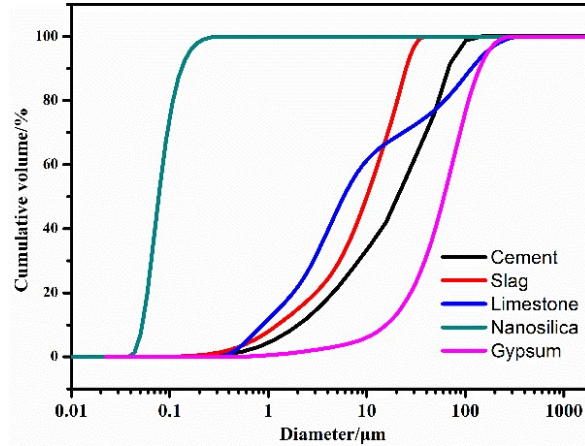
Figure 1. The particle size distribution of the raw materials in this study

2.2. *Preparation of samples*

The formulations of the mixes investigated in this study are shown in **Table 2**. In the four mixes, the clinker and limestone content were kept the same, and the GGBS content varied with the gypsum and NS content, since the amount of GGBS is always abundant. The water to binder (Cement + GGBS + Gypsum + Limestone + NS) ratio (w/b) of all the paste samples was 0.4 and that of all the mortar samples was 0.5 for ensuring the flowability while avoiding bleeding. NS was first dispersed in tap water by ultrasonic dispersion method. For the samples with NS, plasticizer was added to obtain similar fluidity to the samples without NS. The limestone was considered a mineral admixture, and as such its content was maintained at 10%.

After specified durations of standard curing (RH>95%, 20±2°C), paste samples were hydration stopped by immersion in pure isopropanol initially for 24 hours and then in fresh isopropanol for a further 7 days, after which they were dried in a vacuum oven at 40°C for 3 days. The dried hardened pastes were then placed in a vacuum desiccator before characterization by mercury intrusion porosimetry (MIP), X-ray diffraction (XRD), thermal gravity (TG), scanning electron microscopy (SEM).

Table 2. Mixture proportion in this study

| Samples | Clinker | GGBS | Gypsum | Limestone | NS | Superplasticizer | |
						Paste	Mortar
G4	5	81	4	10	-	-	-
G4N3	5	78	4	10	3	1.5	2.5
G10	5	75	10	10	-	-	-
G10N3	5	72	10	10	3	1.5	2.5

103 'G' is for the percentage of gypsum in the SSC, 'N' is for the percentage of NS.

104 *2.3.   Methods*

105 *2.3.1.   Compressive and flexural strength of hardened SSC mortars*

106 In accordance to the Chinese standard 'GB/T 17671-1999', prismatic mortar specimens of

107 4cm×4cm×16cm were made and their compressive and flexural strength were measured at 1, 3, 7, 28,

108 56, and 90 days.

109 *2.3.2.   Porosity of hardened SSC pastes*

110 The porosity of hardened SSC pastes was measured at 90 days by MIP (Micromertics, AutoPore

111 IV 9500). Around 2-3g of dried paste pieces were used for each test. The contact angle was set to 130°.

112 The equilibration time during the intrusion of mercury was 10 seconds. The applied pressure ranged

113 from 0.5 to 55000 psi, corresponding to ~355 um to ~3.3 nm, according to the Washburn's Equation.

114 *2.3.3.   Characterization of hydration products of the SSC pastes*

115 **Quantitative analysis of hydration products**: The quantities of the principal hydration products

116 were estimated using bound water contents, derived from thermal gravimetry. Around 20-30 mg of

117 hydration stopped powdered paste was used for the TGA test, and the mass change recorded over the

118 temperature range 30-1000°C, at a heating rate of 10°C/min, in an argon atmosphere (Flow rate: 50

119 ml/min). The mass loss over the range 50-530°C has been attributed to the bound water within C-(A)-

120 S-H, AFt, gypsum, AFm, and hydrotalcite [3, 7, 24]. Furthermore, the 'tangential method' was used to

121 determine each hydration product following Scrivener et al. [24]. Gypsum shows two water loss peaks

122 on the TG curve[25]. The first is associated with loss of 1.5 water molecules to form calcium sulphate

123 hemihydrate, and the second peak is from removal the last 0.5 molecule to form anhydrite. Only the

124   first peak can be resolved on the TG curve of SSC sample. Therefore, the mass of residual gypsum

125   (M_{Gyp}) can be estimated based on its bound water content (BW_{Gyp}) and the percentage of bound water

126   in gypsum (ω_{Gyp} around 20.9%) by the following formula:

$$M_{Gyp} = \frac{4}{3} BW_{Gyp} / \omega_{Gyp} \tag{1}$$

127   The mass loss over the range 300-500°C was attributed to the bound water of hydrotalcite [3, 7,

128   24]. The mass of hydrotalcite (M_{Ht}) formed upon hydration can be estimated based on its bound water

129   content (BW_{Ht}) and the percentage of bound water in hydrotalcite (ω_{Ht} around 45% [24, 26]) by the

130   following formula:

$$M_{Ht} = BW_{Ht} / \omega_{Ht} \tag{2}$$

131   Bound water in both C-(A)-S-H and AFt is lost at overlapping temperatures. Therefore, selective

132   dissolution with 5$wt.\%$ Na_2CO_3 solution was used to remove the AFt and so as to determine the bound

133   water of the C-(A)-S-H. This was performed according to [7], but with a dry mass of hardened SSC of

134   0.30 ± 0.01 g. The weight loss of the dried residual solid over the range 50-300°C was considered as

135   the bound water content of C-(A)-S-H ($BW_{C\text{-}(A)\text{-}S\text{-}H}$). Based on this, and assuming around 20% bound

136   water in C-(A)-S-H ($\omega_{C\text{-}(A)\text{-}S\text{-}H}$) [24, 26], the mass of C-(A)-S-H produced ($M_{C\text{-}(A)\text{-}S\text{-}H}$) can be estimated

137   by the following formula:

$$M_{C\text{-}(A)\text{-}S\text{-}H} = BW_{C\text{-}(A)\text{-}S\text{-}H} / \omega_{C\text{-}(A)\text{-}S\text{-}H} \tag{3}$$

138   Combining the total weight loss over the range 50-300°C, the bound water content of AFt

139   (BW_{AFt}), gypsum (BW_{Gyp}), the percentage of bound water in AFt (ω_{AFt}, around 45.9% [24, 26]), the

140   mass of AFt (M_{AFt}) produced can be calculated according to the following formula:

$$M_{AFt} = (BW_{Total} - BW_{C\text{-}(A)\text{-}S\text{-}H} - BW_{Gyp}) / \omega_{AFt} \tag{4}$$

141   Because gypsum is not a hydration product, its bound water content should be removed to

142   determine the total bound water associated with hydration. Thus, the total chemical reaction bound

143   water (CBW_{Total}) should be:

$$CBW_{Total} = BW_{Total} - BW_{Gyp} + BW_{Ht} \tag{5}$$

144   Finally, the mass of all the relevant phases (M_{Gyp}, M_{Ht}, $M_{C\text{-}(A)\text{-}S\text{-}H}$, and M_{AFt}) was normalized to

145   the total chemical reaction bound water (CBW_{Total}).

146   **Hydration degree of slag**: Selective dissolution was used to determine the degree of slag

hydration, in accordance with the Chinese standard 'GB/T 12960-2019' [27], which is similar to [7]. Using 0.15 mol/L of EDTA solution, 50 g/L of sodium hydroxide solution, and 33.3*vol.*% of triethanolamine (TEA) solution, 50 mL EDTA solution, 10 mL TEA solution and 120 mL distilled water was added to a 250 mL beaker. Sodium hydroxide solution was then used to adjust the pH to 11.60 ± 0.05. To this solution was added 0.30 ± 0.01 g of dry powder ground to less than 74 μm. The mixture was stirred using a magnetic stirrer for 30 min, after which the insoluble residue was washed with ethanol twice, with suction filtration, and dried in a vacuum oven at 105 ± 5°C for 48 hours. The degree of slag hydration (α_s) was determined by the formula:

$$\alpha_s = 1 - \frac{\frac{W_E}{1 - W_{Wn}} - W_{C,0} W_{C,E}}{W_{S,0} W_{S,E}} \tag{6}$$

Where:

W_E: percentage of residue; W_{Wn}: chemical bound water content (CBW$_{Total}$); $W_{C,0}$: percentage of cement in the mixture; $W_{C,E}$: percentage of residue after the selective dissolution of pure cement; $W_{S,0}$: percentage of slag in the mixture; $W_{S,E}$: percentage of residue after the selective dissolution of slag.

Micro-morphology of the hardened pastes: The morphology of the hydration products, especially AFt, would change with hydration environment (such as the pH value of the pore solution [28]). Therefore, the morphology of the hardened pastes at 90 days was examined by SEM (Guanta FEG 250) with an acceleration voltage of 15 KeV. The test samples were hydration stopped and vacuum dried as mentioned above, and their fresh surface was carbon coated before the test.

To obtain the Ca/(Si+Al) ratios of C-(A)-S-H in different systems, EDS analysis has been on polished samples with an acceleration voltage of 15 KeV. For each sample, 5 different aeras were tested and ten points were selected in one area. Thus, there are 50 data points of Ca/(Si+Al) ratios for one sample, from which a value with a maximum probability was obtained.

3. Results

3.1. Mechanical property of hardened SSC mortars

171
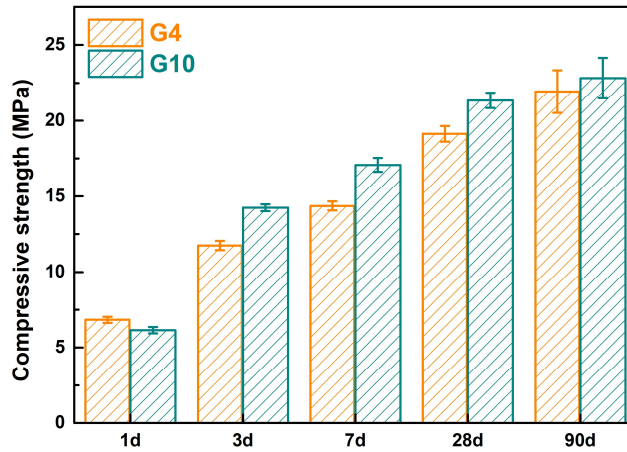
Figure 2 present the compressive strength respectively of SSC with different gypsum contents. There was a gradual increase in compressive strength over time, with the samples prepared with 10% gypsum (G10) showing slightly higher compressive strengths at all ages apart from at 1 day. However, the effect of gypsum content on compressive strength was less clear cut, as pointed out by Luz et al. [29].

177
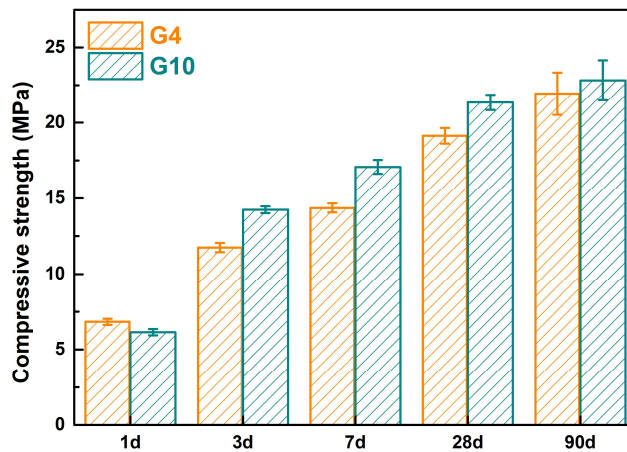
Figure 2. Compressive strength of SSC with different gypsum content as a function of time

Figure 3 a and b present the influence of NS on the compressive strength of hardened SSC mortars. Irrespective of gypsum content, the addition of NS led to a significant increase in compressive strength. While sample G4 (4% gypsum by weight) only attained a strength of ~22 MPa, even after 90 days, this doubled upon addition of 3% NS. The effect was slightly less pronounced for sample G10, but the addition of NS still had a significant positive impact. **Figure 3** a and b also show the compressive strength ratio between the samples prepared with and without NS. The positive effect of NS addition increases with curing age. The phenomenon is obviously different from the effect of NS in Portland cement system and blend cement system, in which, NS mainly improves early-age mechanical

performance (i.e. the first 7 days) by filling effect and nucleation seeding effect, and pozzolanic reaction [17].
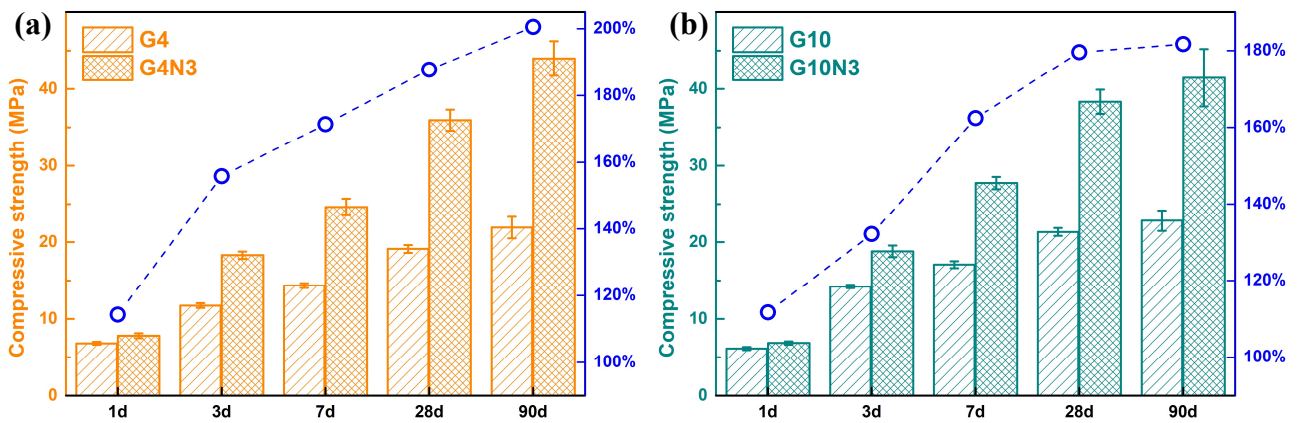
Figure 3. Influence of NS on the compressive strength of SSC with (a) 4% and (b) 10% gypsum

3.2. Microstructure of hardened SSC pastes

3.2.1. Porosity of hardened SSC pastes

It has been shown that the pore structure of materials is closely related to their compressive strength, with a lower porosity correlating with higher compressive strength [30]. Since NS significantly enhances SSC compressive strength (**Figure 3**a and b), it is expected that these SSC systems will also show a refined pore structure. This was confirmed by mercury intrusion porosimetry (**Figure 4** a and b).
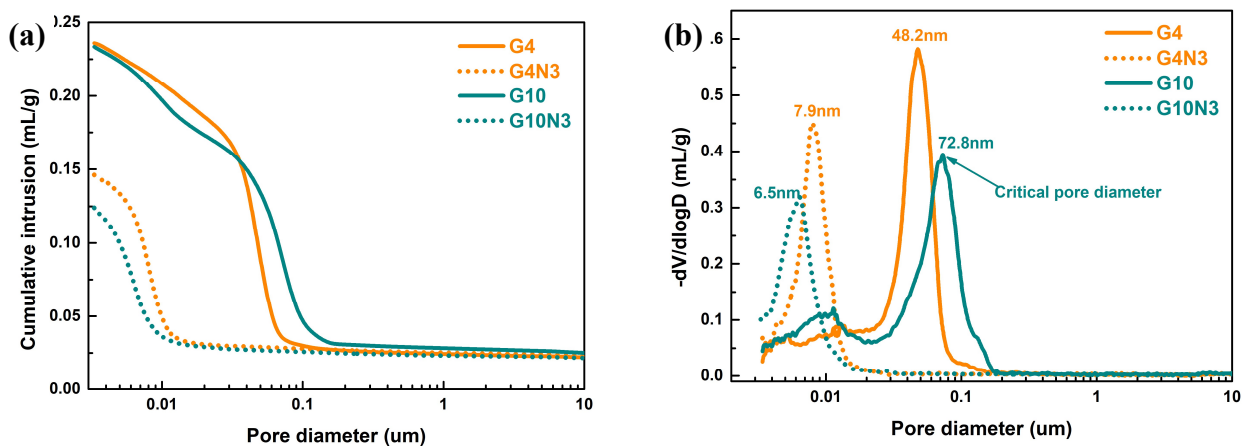
Figure 4. (a) Porosities and (b) pore distributions of different hardened SSC pastes at 90 days

Addition of 3% NS decreased the cumulative mercury intrusion of the 90-day hardened samples from around 0.23 mL/g (G4 and G10) to less than 0.15 mL/g (G4N3 and G10N3). Taking these values,

201   the calculated porosity of G4 and G10 was reduced from 34.1 (G4) and 32.0% (G10) to 20.2% (G4N3)

202   and 19.5% (G10N3). Furthermore, as shown in **Figure 4**b, the critical pore diameter of the hardened

203   samples reduced significantly, from 48.2 nm (G4) and 72.8 nm (G10) to 7.9 nm (G4N3) and 6.5 nm

204   (G10N3); a reduction of 83.6% and 91.0%, respectively. The refinement of pore structure by well-

205   dispersed NS in Portland cement-based materials has been widely reported [31-33]. This is frequently

206   attributed to a combination of the filler effect, pozzolanic reactions, and the seeding effect [18, 32, 34].

207   However, since only traces of calcium hydroxide are formed in supersulfated cement system due to

208   their very low Portland cement contents [9], the pozzolanic reaction is unlikely to be a significant

209   reason for the densifying effect of NS. However, the interaction between NS and aluminate [21] could

210   play a critical role in the hydration of slag, the main component of SSC, as elaborated in section 3.3.

211

212   *3.2.2. Morphology of hardened SSC pastes*

213   The morphology of the hardened SSC samples prepared with 4% gypsum is presented in **Figure**

214   **5**. The overall structure of G4 is pretty porous (**Figure 5** a and b), whereas that of G4N3 is much denser

215   (**Figure 5** c and d). This is consistent with the MIP data shown earlier (**Figure 4** a and b). In addition,

216   the AFt needles in G4 are thinner (approximately 0.25 microns) than those in G4N3 (approximately

217   1.09 microns), as shown in **Figure 7**. Ma et al. [19] reported a similar effect in calcium aluminate

218   cements, with NS leading to shorter and thicker AFt crystals.

219   The morphology of the hardened SSC samples with 10% gypsum is presented in **Figure 6**.

220   Comparing **Figure 6** a and b with **Figure 5** a and b, it can be seen that gypsum content has little impact

221   on morphology. But, **Figure 6** c and d show that the addition of NS densifies the microstructure of

222   samples with higher gypsum contents just as for lower gypsum contents.
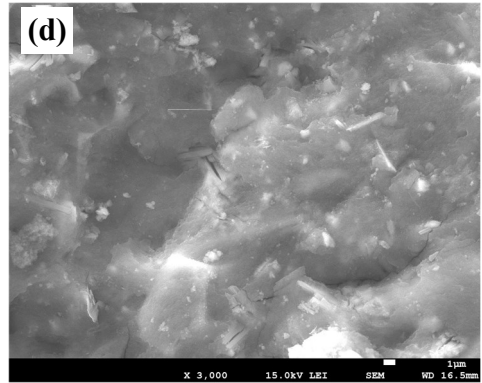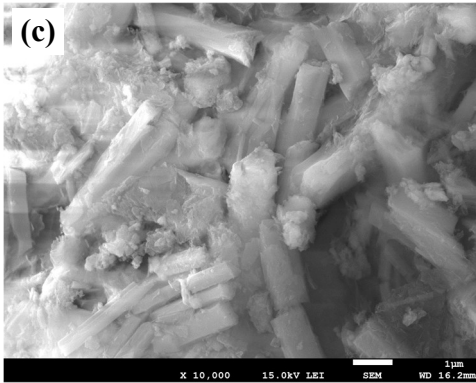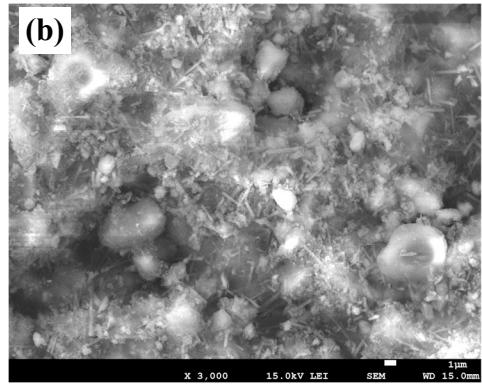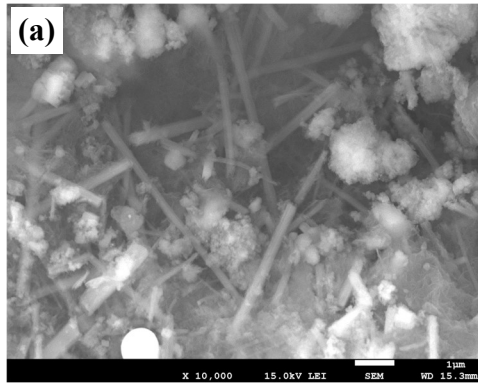
223   **Figure 5.** Micromorphology of (a, b) G4 and (c, d) G4N3 at 90 days
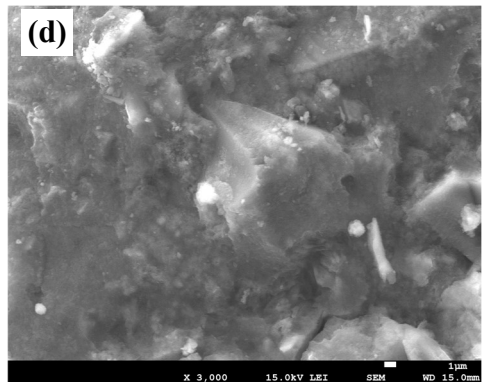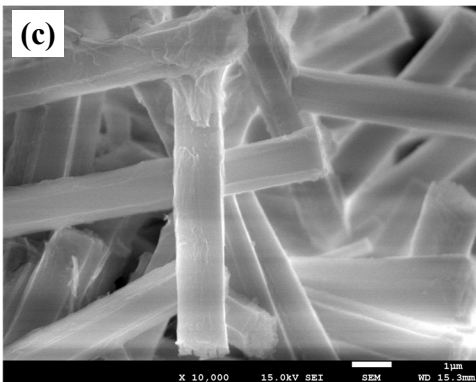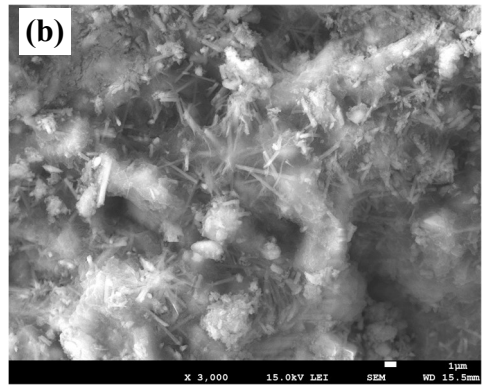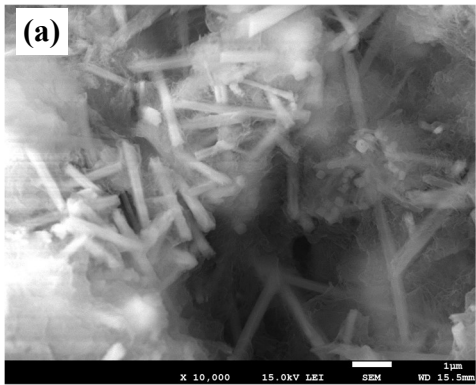
224   **Figure 6.** Micromorphology of (a, b) G10 and (c, d) G10N3 at 90 days

225
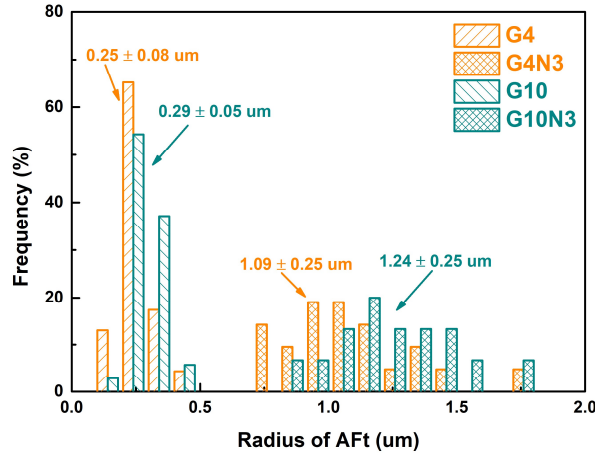
Figure 7. Radius of AFt in different samples

3.2.3. Ca/(Si+Al) of C-(A)-S-H of hardened SSC pastes

C-(A)-S-H is one of the principal hydration products, and its composition and structure play an important role in the performance of hardened pastes. It was found that the C-S-H with lower Ca/Si (from 0.7 to 2.1) has higher elastic modulus and hardness [35]. Kunther et al. [36] found that the compressive strength of C-S-H increased with the decreasing of Ca/Si.

Figure 8 presents the influence of NS on the Ca/(Si+Al) of C-(A)-S-H in the hardened pastes. It can be found that the Ca/(Si+Al) of C-(A)-S-H in the SSC system is smaller than that of Portland cement, which is consistent with Thomas et al. [9]. With the addition of NS, the Ca/(Si+Al) of C-(A)-S-H was reduced to around 1.0 as shown in **Figure 8** b,d, contributing to the higher performance of system with NS.

238

239 *3.3. Phase assemblages of hardened SSC pastes*

240 The phase assemblage of hardened pastes is a key factor dictating the SSC performance

241 (including compressive strength). Therefore, the consumption of both gypsum and slag, plus the

242 production of AFt and C-(A)-S-H was explored.
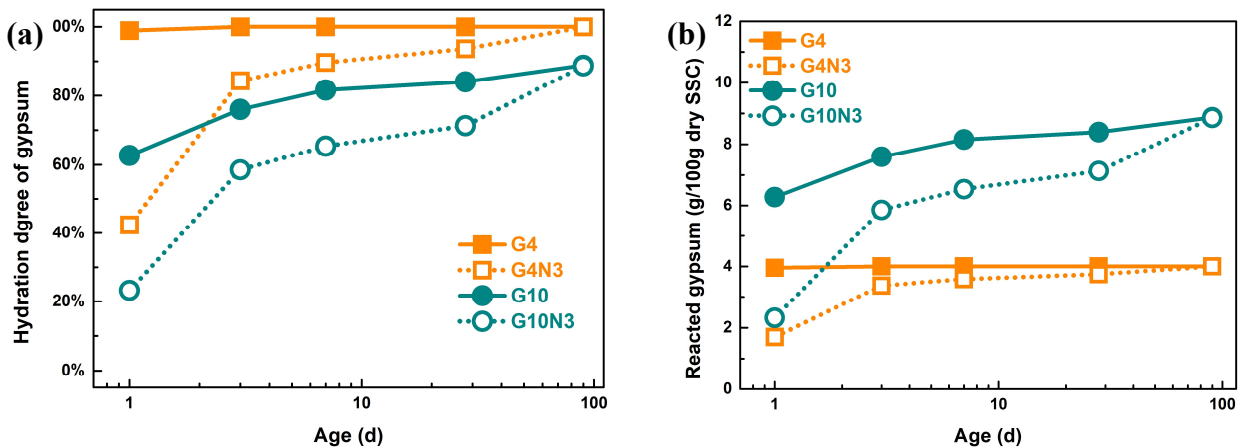
243 **Figure 9.** (a) Hydration degree and (b) quantity of reacted gypsum as a function of time

244 **Figure 9**a shows the degree of gypsum consumption over time. Gypsum was almost completely

245 consumed in sample G4 within 1 day. Meanwhile, gypsum consumption was significantly hindered by

246 the addition of NS, with 40% consumed by 1 day in G4N3 (2g/100g SSC as shown in **Figure 9**b), and

247 complete consumption only by 90 days. The same trend was seen for the samples prepared with 10%

248 gypsum (G10 and G10N3). The inhibiting effect of NS has been found by the authors' previous study

249 on the C_3A+Gypsum system [21].

250 Comparing the extent of gypsum consumption in the samples without NS (G4 and G10), (**Figure**

251 **9**b) suggests that 4% gypsum might be insufficient, since 6 g/100g SSC was consumed within 1 day

252　in sample G10. For the samples containing NS (G4N3 and G10N3), (**Figure 9**b), gypsum consumption

253　was faster with higher gypsum contents, indicating that the rate of gypsum consumption is related to

254　the gypsum content.

255　　　Gypsum is consumed during the reaction with aluminates in the slag, resulting in AFt generation.

256　This is a key factor dictating the compressive strength of hardened SSC [9]. Therefore, the amount of

257　AFt was tracked as a function of time, (**Figure 10**), and there was a clear correlation between AFt

258　contents and the consumption of gypsum, as shown in **Figure 9**b. The addition of NS delayed the

259　generation of AFt, but the final AFt content was determined by the initial gypsum content. The results

260　also indicate that, counter to conventional understanding, the amount of AFt is not the only determinant

261　of compressive strength in the systems with NS, since these samples develop much higher compressive

262　strengths than those without NS.
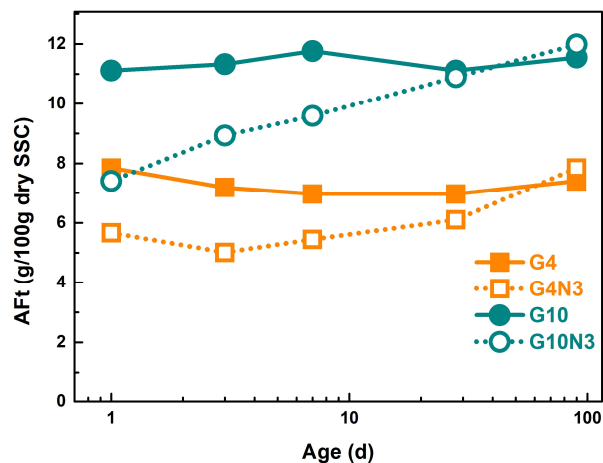
263

264　　　　　　　　　　　**Figure 10.** Evolution of AFt as a function of time

265　　　Considering that the aluminate for AFt production is from the dissolution of slag, one would

266　expect that the extent of slag dissolution would correlate with that of both gypsum consumption

267　(**Figure 9**b) and AFt generation (**Figure 10**). However, **Figure 11**, which presents the degree of slag

268　hydration as a function of time, suggests that this seems not to be the case. The degree of slag hydration

269　in the samples with NS is much larger than that without NS after 7 days (**Figure 11**), illustrating the

270　key role of NS in promoting slag hydration. Although gypsum consumption was proportional to its

271　content (**Figure 9**b) and rate of AFt production (**Figure 10**), it only slightly increases the degree of

272　slag hydration.
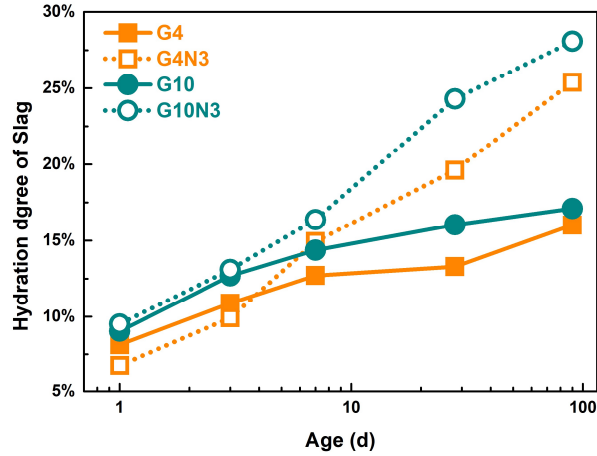
Figure 11. Degree of slag hydration as a function of time

There, at first, appears to be a contradiction in the role of NS; promoting the hydration of SSC (**Figure 11**), yet delaying the formation of AFt (**Figure 10**). What happens to the aluminate released upon slag dissolution in the presence of NS? One possible reason could be incorporation in C-(A)-S-H. The formation of C-(A)-S-H has been considered as the main reason for the long-term strength enhancement [9]. **Figure 12** shows the amount of C-(A)-S-H (determined by the TG method mentioned above) formed in each system over time, highlighting the effect of NS addition. The addition of NS increases C-(A)-S-H content, particularly at later age. the formation of C-(A)-S-H provides a sink for aluminate ions released upon slag dissolution [26]. It has long been proposed that NS provides nucleation sites [18] and so promotes C-S-H formation in the Portland cement-based materials [37, 38]. Here in super sulfated cement systems, NS seems to have a similar effect on the formation of C-(A)-S-H.
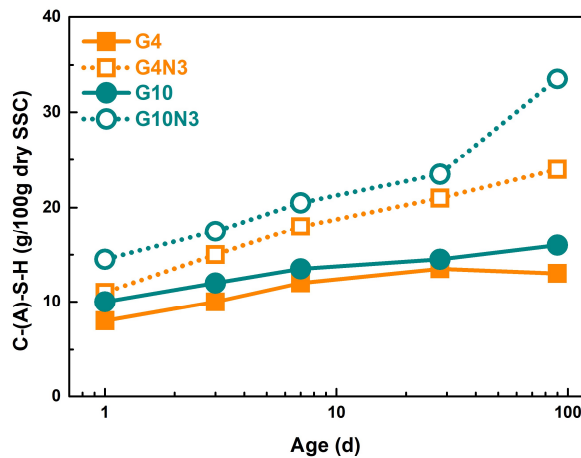
Figure 12. Evolution of C-(A)-S-H in the hardened SSC with time

15

4. Discussion

4.1. The factors determining the strength development of SSC

Since slag hydration leads to formation of C-(A)-S-H and in the presence of gypsum, AFt, then the degree of slag hydration should be closely related to the compressive strength of SSC. It should be noted that the slag contents of the four mixtures (G4, G4N3, G10, G10N3) are slightly different (see **Table 2**). Thus, while the degree of slag hydration tells us about the reaction kinetics, quantifying the amount of reacted slag could be a more suitable parameter relating to the compressive strength. This is clearly demonstrated in **Figure 13**, with compressive strength increasing almost linearly with the amount of reacted slag. However, there is a distinction between the samples without NS (G4 and G10) and with NS (G4N3 and G10N3), but no dependence on gypsum content. For a given quantity of reacted slag, samples containing NS showed slightly higher strengths than those without.
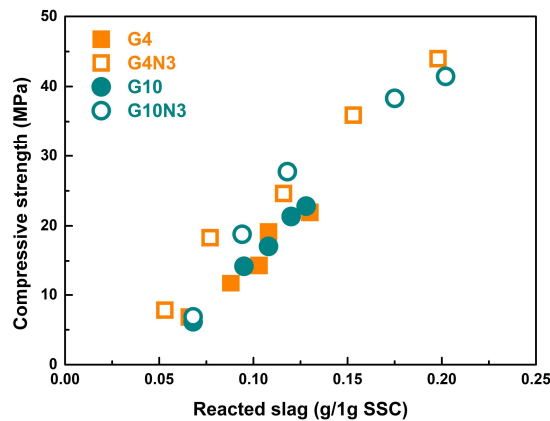
Figure 13. Compressive strength development of SSC as a function of reacted slag

The primary effect of NS on the hardened SSC is its promotion of C-(A)-S-H growth (**Figure 12**) and its inhibition of AFt growth (**Figure 10**). Thus, use of NS increases the volume ratio of C-(A)-S-H to AFt. It has been found that this ratio is a key factor affecting the compressive strength of sulfoamuminate cements [39]. Through the assumption of the density of C-(A)-S-H (2.48 g/cm^3 [40], some others proposed to be 2.6 g/cm^3 [41], 2.7 g/cm^3 [42]) and AFt (1.78 g/cm^3 [40]), the volume ratio and distribution could be calculated readily. It can be seen from **Figure 14**a that addition of NS lowers the AFt/C-(A)-S-H ratio. In addition, the compressive strength of SSC decreases with the ratio of AFt/C-(A)-S-H, as shown in **Figure 14**b.

16
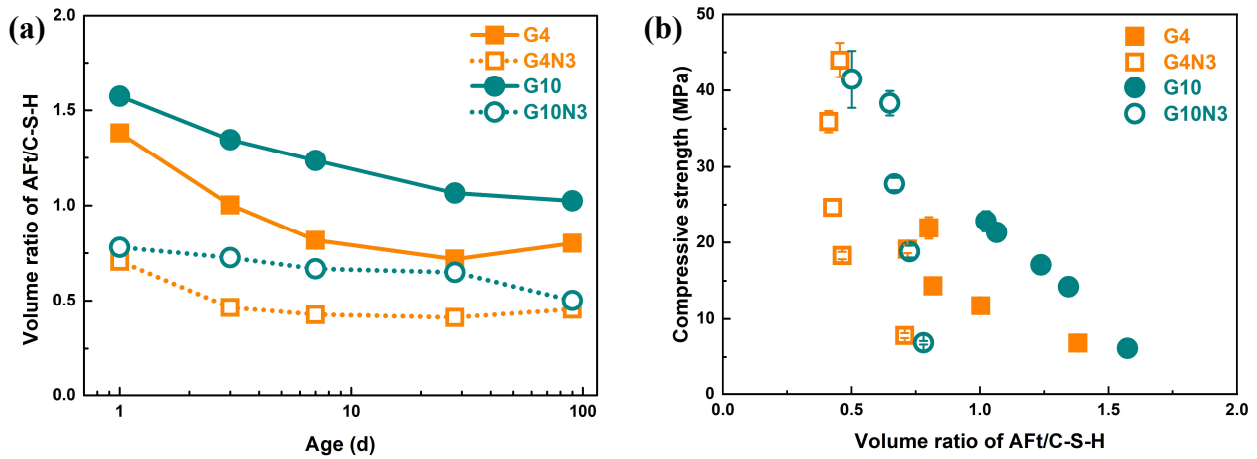
Figure 14. (a) Volume ratio of AFt/C-(A)-S-H as a function of time and (b) its relation with

310 the compressive strength of SSC

311   Based on the analysis above, it can be seen that the amount of reacted slag and the volume ratio

312 of AFt/C-(A)-S-H in the hardened SS are two important factors affecting the compressive strength.

313 Therefore, the compressive strength was assumed to be predicted with the formula: $S = A\alpha^n/\beta^m + \gamma$,

314 where α denotes the reacted slag; β denotes the volume ratio of AFt/C-(A)-S-H. **Figure 15** presents

315 the fitting result and the comparison between the measured and predicted compressive strength. The

316 regression coefficient is 0.94, indicating a good fit.

Prediction function:
Strength=$169.9\alpha^{0.575}/\beta^{0.172}$-22.9
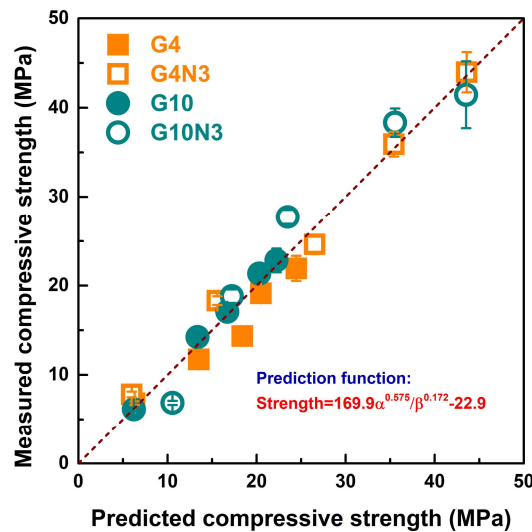
317

318   **Figure 15.** Comparison between the measured and the predicted compressive strength

319 *4.2.   The role of gypsum in the compressive strength development of SSC*

320   Gypsum is a key component of SSC. Its obvious contribution is in promoting the formation of

321 AFt (Figure 9). However, higher gypsum contents also increase the degree of slag hydration (**Figure**

11a), thus increasing the quantity of C-(A)-S-H (**Figure 12**). The formation of additional AFt and C-(A)-S-H will affect the volume ratio of AFt/C-(A)-S-H (**Figure 14**a). It seems that the enhancing effect of higher gypsum content in accelerating the consumption of slag is partially counteracted by its negative effect through the increase in volume ratio of AFt/C-(A)-S-H.

While not a primary focus of this study, it should be noted that the carbonation resistance of C-S-H is much higher than that of AFt [43]. Therefore, it could be expected that a lower AFt/C-(A)-S-H ratio could improve the carbonation resistance of SSC. So, the gypsum content of SSC could play an important role in the carbonation resistance of SSC, which is part of the ongoing work of the authors.

4.3.   The role of NS in the compressive strength development of SSC

There are two other important impacts of NS on the compressive strength of SSC, except the filling effect as found in the Portland cement [33]. One is the reduction in the AFt/C-(A)-S-H volume ratio (see **Figure 14**a), the other is promotion of slag hydration (see **Figure 11**a). Although NS has been shown here to increase the compressive strength at all ages, different factors are at work during different stages. During the first 7 days, incorporation of NS inhibits AFt formation (see **Figure 10**) and may impede slag hydration when lower gypsum levels are used (see **Figure 11**b). However, over time it increases the amount of C-(A)-S-H (see **Figure 12**) and reduces the AFt/C-(A)-S-H volume ratio (see **Figure 14**a). The higher volume ratio over the first 7 days is the main reason for the higher compressive strength of samples containing NS. Beyond 7 days, samples containing NS show elevated slag hydration and lower AFt/C-(A)-S-H volume ratios, both of which contribute to the enhancement of compressive strength.

However, what is the reason for the increase in reacted slag by NS? It can be seen from **Figure 11**a,b that the degree of slag hydration in the presence of NS increases linearly to 90 days, while in the absence of NS, hydration levels off after 7 days. Thus, something inhibits long-term slag hydration in the systems without NS.

The following several factors are possible reasons. ***First*** is the available water for slag hydration. It should be noted that 1 g of AFt contains 0.459 g of water and 1g of C-S-H ($C_{1.7}SH_2$, as in [24]) contains 0.189g of water. Therefore, for every gram of AFt not formed, there is sufficient water to form 2.4 g of C-S-H (0.459/0.189=2.4). Since in the systems containing NS, the formation of AFt is inhibited

350 (see **Figure 10**), and the AFt/C-(A)-S-H volume ratio is reduced (see **Figure 11**b), with a fixed amount

351 of mixing water, more hydration products could be formed in the systems containing NS. ***Second*** is

352 the available space for hydrate growth. The density of C-(A)-S-H is greater than that of AFt [40], and

353 the addition of NS will increase the degree of polymerization of C-(A)-S-H [44] which will increase

354 the density of C-(A)-S-H further [36, 45]. Thus, the lower AFt/C-(A)-S-H volume ratio associated with

355 NS addition will lead to a higher overall density of hydration products, allowing greater slag hydration

356 at later ages. ***Third*** is the distribution of C-(A)-S-H. At hydration proceeds, the diffusion of ions

357 released from slag dissolution could be a limiting factors, as in Portland cement systems [46]. It has

358 been shown that the long-term strength of SSC is determined by the formation of C-(A)-S-H [9].

359 However, diffusion of silicate ions is slow, especially at lower pH [47]. It has been proposed that at

360 lower pH, there exists a layer enriched in Si and Al around the dissolving slag [47]. In this situation,

361 C-(A)-S-H would be precipitated around the slag particles, and the diffusion of free water to the surface

362 of the slag will be slowed. Nevertheless, in the system with NS, the evenly distributed NS will provide

363 many nucleation sites for C-(A)-S-H [37], and promote the precipitation of silicate ions released upon

364 slag dissolution. This would create a silicate sink, preventing the accumulation of an encasing C-(A)-

365 S-H layer around the slag particles. ***Fourth*** is the pore solution chemistry of the system, since it

366 provides the driving force of the hydration reaction, however, the thermodynamic and kinetic

367 modelling analysis would be dictated in the author's following contribution.

5. Conclusions

369   The SSC, containing about 5% Portland cement, is a classic low-carbon cement. However, its low

370 early-age strength has been one of the factors limiting its practical application. In this study, NS was

371 added into the SSC system, aimed at improving its mechanical properties by promoting the

372 precipitation of C-(A)-S-H. Based on the analysis above, it can be concluded that:

373   (1) The addition of NS increases the early- (3 days) and late-age (90 days) compressive strength

374 by 35%-60% and 80%-100%, respectively. There is also a significant reduction in critical pore size.

375 Meanwhile, the gypsum content of SSC has little influence on the relevant properties.

376   (2) The compressive strength of SSC is linearly correlated with the amount of reacted slag more

377 than the hydration degree of slag.

378   (3) The level of reacted slag in the SSC continued to increase throughout the duration of the study

379 (90 days) when NS was added, but levelled off after 7 days in the absence of NS.

380   (4) The addition of NS slows down the consumption of gypsum and the formation of AFt, but

381 does not affect their final levels. However, NS does both accelerate the formation of C-(A)-S-H and

382 increase the total amount formed, reducing the AFt/ C-(A)-S-H volume ratio.

383   (5) Use of higher gypsum contents increases the consumption rate of gypsum and the total amount

384 of AFt generated. However, it barely affects the slag hydration.

385   (6) The amount of reacted slag (α) and AFt/ C-(A)-S-H volume ratio (β) are two important factors

386 dictating the compressive strength (S) of hardened SSC mortars. In this study, their relation may be

387 represented by the formula: $S = 169.9\alpha^{0.58}/\beta^{0.17} - 22.9$.

388   This work proves the significant positive benefits of NS on the performance of SSC and highlights

389 the critical role of silicate and aluminate relation kinetics in the hydration of SSC, providing a new

390 perspective for improving performance of SSC.

391

402

Compliance with ethical standards

Conflict of interest The authors declare that they have no conflicts of interest.

References

1. Juenger, M.C.G., et al., *Advances in alternative cementitious binders.* Cement and Concrete Research, 2011. **41**(12): p. 1232-1243.

2. Wu, Q., Q. Xue, and Z. Yu, *Research status of super sulfate cement.* Journal of Cleaner Production, 2021. **294**: p. 126228.

3. Masoudi, R. and R.D. Hooton, *Influence of alkali lactates on hydration of supersulfated cement.* Construction and Building Materials, 2020. **239**: p. 117844.

4. Liu, S., J. Ouyang, and J. Ren, *Mechanism of calcination modification of phosphogypsum and its effect on the hydration properties of phosphogypsum-based supersulfated cement.* Construction and Building Materials, 2020. **243**: p. 118226.

5. Gracioli, B., et al., *Influence of the calcination temperature of phosphogypsum on the performance of supersulfated cements.* Construction and Building Materials, 2020. **262**: p. 119961.

6. Winnefeld, F. and B. Lothenbach, *Hydration of calcium sulfoaluminate cements — Experimental findings and thermodynamic modelling.* Cement and Concrete Research, 2010. **40**(8): p. 1239-1247.

7. Masoudi, R. and R.D. Hooton, *Examining the hydration mechanism of supersulfated cements made with high and low-alumina slags.* Cement and Concrete Composites, 2019. **103**: p. 193-203.

8. Gruskovnjak, A., et al., *Hydration mechanisms of super sulphated slag cement.* Cement and Concrete Research, 2008. **38**(7): p. 983-992.

9. Matschei, T., F. Bellmann, and J. Stark, *Hydration behaviour of sulphate-activated slag cements.* Advances in Cement Research, 2005. **17**: p. 167-178.

10. Richardson, I.G., et al., *The characterization of hardened alkali-activated blast-furnace slag*

pastes and the nature of the calcium silicate hydrate (C-S-H) phase. Cement and Concrete Research, 1994. **24**(5): p. 813-829.

11. Zhou, Y., et al., *The influence of two types of alkali activators on the microstructure and performance of supersulfated cement concrete: mitigating the strength and carbonation resistance.* Cement and Concrete Composites, 2021. **118**: p. 103947.

12. Briki, Y., et al., *Factors affecting the reactivity of slag at early and late ages.* Cement and Concrete Research, 2021. **150**: p. 106604.

13. Scrivener, K.L., P. Juilland, and P.J.M. Monteiro, *Advances in understanding hydration of portland cement.* Cement and Concrete Research, 2015. **78**: p. 38-56.

14. Bullard, J.W., G.W. Scherer, and J.J. Thomas, *Time dependent driving forces and the kinetics of tricalcium silicate hydration.* Cement and Concrete Research, 2015. **74**: p. 26-34.

15. Land, G. and D. Stephan, *The effect of synthesis conditions on the efficiency of C-S-H seeds to accelerate cement hydration.* Cement and Concrete Composites, 2018. **87**: p. 73-78.

16. Yu, J., et al., *Effect of ettringite seed crystals on the properties of calcium sulphoaluminate cement.* Construction and Building Materials, 2019. **207**: p. 249-257.

17. Liu, X., P. Hou, and H. Chen, *Effects of nanosilica on the hydration and hardening properties of slag cement.* Construction and Building Materials, 2021. **282**: p. 122705.

18. Land, G. and D. Stephan, *The influence of nano-silica on the hydration of ordinary Portland cement.* Journal of Materials Science, 2011. **47**(2): p. 1011-1017.

19. Ma, B., et al., *Influence of nano SiO_2 on the hydration and hardening of sulfoaluminate cement (in Chinese).* Journal of Functional Materials, 2016. **47**(02): p. 2010-2014.

20. Li, G., et al., *Characteristic of silica nanoparticles on mechanical performance and microstructure of sulphoaluminate cement/ordinary Portland cement binary blends.* Construction and Building Materials, 2020. **242**.

21. Hou, P., et al., *Physicochemical effects of nanosilica on C_3A/C_3S hydration.* Journal of the American Ceramic Society, 2020. **103**(11): p. 6505-6518.

22. Adu-Amankwah, S., et al., *Influence of limestone on the hydration of ternary slag cements.* Cement and Concrete Research, 2017. **100**: p. 96-109.

458   23.   De Weerdt, K., et al., *Synergy between fly ash and limestone powder in ternary cements.*

459   Cement and Concrete Composites, 2011. **33**(1): p. 30-38.

460   24.   Scrivener, K., R. Snellings, and B. Lothenbach, *A Practical Guide to Microstructural Analysis*

461   *of Cementitious Materials.* 2015.

462   25.   Li, B., et al., *GGBS hydration acceleration evidence in supersulfated cement by nanoSiO$_2$.*

463   Cement and Concrete Composites, 2022. **132**: p. 104609.

464   26.   Lothenbach, B. and A. Nonat, *Calcium silicate hydrates: Solid and liquid phase composition.*

465   Cement and Concrete Research, 2015. **78**: p. 57-70.

466   27.   *Quantitative determination of constituents of cement.* 2019, Standards Press of China: Beijing.

467   28.   Min, D. and T. Mingshu, *Formation and expansion of ettringite crystals.* Cement and Concrete

468   Research, 1994. **24**(1): p. 119-126.

469   29.   Luz, C.A.d. and R.D. Hooton, *Influence of Supersulfated Cement Composition on Hydration*

470   *Process.* Journal of Materials in Civil Engineering, 2019. **31**(6): p. 04019090.

471   30.   Chen, X., S. Wu, and J. Zhou, *Influence of porosity on compressive and tensile strength of*

472   *cement mortar.* Construction and Building Materials, 2013. **40**: p. 869-874.

473   31.   Li, G., *Properties of high-volume fly ash concrete incorporating nano-SiO2.* Cement and

474   Concrete Research, 2004. **34**(6): p. 1043-1049.

475   32.   P. P, A., et al., *Effect of nano-silica in concrete: a review.* Construction and Building Materials,

476   2021. **278**: p. 122347.

477   33.   Said, A.M., et al., *Properties of concrete incorporating nano-silica.* Construction and Building

478   Materials, 2012. **36**: p. 838-844.

479   34.   Singh, L.P., et al., *Beneficial role of nanosilica in cement based materials - A review.*

480   Construction and Building Materials, 2013. **47**: p. 1069-1077.

481   35.   Pelisser, F., P.J.P. Gleize, and A. Mikowski, *Effect of the Ca/Si Molar Ratio on the*

482   *Micro/nanomechanical Properties of Synthetic C-S-H Measured by Nanoindentation.* The

483   Journal of Physical Chemistry C, 2012. **116**(32): p. 17219-17227.

484   36.   Kunther, W., S. Ferreiro, and J. Skibsted, *Influence of the Ca/Si ratio on the compressive*

485   *strength of cementitious calcium–silicate–hydrate binders.* Journal of Materials Chemistry A,

486   2017. **5**(33): p. 17401-17412.

487   37.   Hou, P.K., et al., *Modification effects of colloidal nanoSiO(2) on cement hydration and its gel*
488   *property.* Composites Part B-Engineering, 2013. **45**(1): p. 440-448.

489   38.   Sanchez, F. and K. Sobolev, *Nanotechnology in concrete – A review.* Construction and Building
490   Materials, 2010. **24**(11): p. 2060-2071.

491   39.   Li, J., *Study on the sintering and hydration mechanism of a $C_4A_3\$-C_2S$ binary system (in*
492   *Chinese).* 2019.

493   40.   Lothenbach, B., et al., *Cemdata18: A chemical thermodynamic database for hydrated Portland*
494   *cements and alkali-activated materials.* Cement and Concrete Research, 2019. **115**: p. 472-506.

495   41.   Thomas, J.J., H.M. Jennings, and A.J. Allen, *Relationships between Composition and Density*
496   *of Tobermorite, Jennite, and Nanoscale CaO−SiO2−H2O.* The Journal of Physical Chemistry
497   C, 2010. **114**(17): p. 7594-7601.

498   42.   Muller, A.C.A., et al., *Densification of C–S–H Measured by 1H NMR Relaxometry.* The Journal
499   of Physical Chemistry C, 2012. **117**(1): p. 403-412.

500   43.   Steiner, S., et al., *Effect of relative humidity on the carbonation rate of portlandite, calcium*
501   *silicate hydrates and ettringite.* Cement and Concrete Research, 2020. **135**.

502   44.   Sousa, M.I.C. and J.H.d.S. Rêgo, *Effect of nanosilica/metakaolin ratio on the calcium alumina*
503   *silicate hydrate (C-A-S-H) formed in ternary cement pastes.* Journal of Building Engineering,
504   2021. **38**: p. 102226.

505   45.   Gallucci, E., X. Zhang, and K.L. Scrivener, *Effect of temperature on the microstructure of*
506   *calcium silicate hydrate (C-S-H).* Cement and Concrete Research, 2013. **53**: p. 185-195.

507   46.   Bullard, J.W., et al., *Mechanisms of cement hydration.* Cement and Concrete Research, 2011.
508   **41**(12): p. 1208-1223.

509   47.   Skibsted, J. and R. Snellings, *Reactivity of supplementary cementitious materials (SCMs) in*
510   *cement blends.* Cement and Concrete Research, 2019. **124**: p. 105799.

511